Natural fibres actuators for smart bio-inspired hygromorph biocomposites

Antoine Le Duigou[a], Samuel Requile[a], Johnny Beaugrand[b,c], Fabrizio Scarpa[d] and Mickael Castro[a]

[a] Univ. Bretagne Sud, FRE CNRS 3744, IRDL, F-56100 Lorient, France

[b] Biopolymères Interactions Assemblages (BIA), INRA, rue de la Géraudière, F-44316 Nantes, France

[c] FARE Laboratory, INRA, Université de Reims Champagne-Ardenne, F-51100 Reims, France

[d] Bristol Composites Institute (ACCIS), University of Bristol, BS8 1TR Bristol, UK

***corresponding author:**
Antoine.le-duigou@univ-ubs.fr
Tel: +33297874586

Fax: +33297874588

Abstract:

Hygromorph biocomposite (HBC) actuators make use of the transport properties of plant fibres to generate an out-of-plane displacement when a moisture gradient is present. HBC actuators possess a design based on the bilayer configuration of natural hygromorph actuators (like Pine cone, Wheat awn, *Selaginella lepidophyll*). In this work we present a series of design guidelines for HBCs with improved performance, low environmental footprints and high durability in severe environments. We develop a theoretical actuating response (curvature) formulation of Maleic Anhydride PolyPropylene (MAPP)/plant fibres based on bimetallic actuators theory. The actuation response is evaluated as a function of the fibre type (flax, jute, kenaf and coir). We demonstrate that the actuation is directly related to the fibre microstructure and its biochemical composition. The jute and flax fibres appear to be the best candidates for use in HBCs. Flax/MAPP and jute/MAPP HBCs exhibit similar actuating behaviours during the sorption phase (amplitude and speed), but different desorption characteristics due to the combined effect of the lumen size, fibre division and biochemical composition on the desorption mechanism. During hygromechanical fatigue tests the jute/MAPP HBCs exhibit a drastic improvement in durability compared to their flax counterparts. We also provide a demonstration on how HBCs can be used to trigger deployment of more complex structures based on Origami and Kirigami designs.

Keywords: Natural fibres, biocomposite, actuator, moisture, morphing

1 Introduction

Deployable structures are in general actuated by using a mechanical or a multiphysics stimulus. Researchers have recently investigated the feasibility of developing autonomous self-shaping structures with integrated smart materials (such as shape memory alloys or polymers [1][2]) to reduce

the complexity of the systems. The change of temperature is an example of the stimulus used in these shape memory materials to generate the morphing of the structure for deployment. Unlike metals, shape memory polymers have low density and are easy to process and customize. To enhance the deployment performance, Origami and Kirigami design strategies can be also adopted, as they enable the transformation of 2D sheets into three-dimensional deployable configurations [3]. These two design paradigms can also be used to produce deployable cellular materials, in which the final honeycomb geometry can be well predicted from the folding and/or cutting pattern [4][5].

The natural environment is however complex, and a pure temperature variation may not be sufficient to guarantee an actuation since temperature and humidity tend to superimpose their contributions. Humidity is however rarely discussed as a potential stimulus for deployment systems [3][6][7], aside from cases related to the self-folding of hydrogel-based micro-actuators [8], electrically activated papers [9], or paper based respiration sensors [10].

In recent years different research groups have developed hygromorph biocomposites (HBCs), with designs inspired by the bilayer microstructure of natural hydraulic actuators (e.g., pine cones [11][12]). The bilayer configuration allows the triggering of an out-of-plane displacement response when a moisture gradient is present. Contrary to synthetic actuating fibres [8], HBCs represent a disruptive approach to use plant fibres and their natural actuation potential [11][13][14][15]. HBCs are also inexpensive, locally available and environmentally friendly. The development and use of hygromorph biocomposites also potentially opens different sets of applications for natural fibre producers, enabling them to diversify the market share away from the traditional textile industry. Plant fibres exhibit high water sensitivity and transverse swelling, which is currently considered as a major impediment to their industrial development [16]. When plant fibres are used in asymmetric (bilayer-like) laminates, their anisotropic swelling induces the formation of a curvature because of the formation of hygroscopic stresses. Plant fibres function in this case as hygroscopically active building blocks, rather than as a simple polymer reinforcement material.

The actuation of a moisture-induced actuator can be programmed through the swelling coefficient, the moisture content, the stiffness or the thickness ratio [17][18]. Previous works related to flax fibre/polypropylene (PP) hygromorph actuators have shown that the response not only depends upon the fibre volume content, but also on the interfacial shear strength [15]. Nevertheless, the durability of these actuators in severe environments like water immersion is limited by the mechanical degradation. In this case, polysaccharides leachate and porosity are produced due to existing swelling/shrinking processes and the delamination occurring between layers [14][15][19][20][21]. HBCs can also actuate in environments where the variation of moisture occurs with or without an

accompanying temperature change. HBCs can be therefore used as a deploying system as a whole, or as building block for deployment, like an active hinge for self-shaping devices.

Natural reinforcements such as bast (e.g., flax, hemp, jute, or kenaf) and fruit fibres (coir) are derived from local feedstocks, which feature a moderate environmental footprint [22] and potential recyclability and compostability at their end of life. As a natural system, plant fibres have an intrinsic complex and relation between hierarchical form and functionality. For example, bast fibres have a primary role as stem reinforcement, but also possess a hierarchical structure with a low microfibrillar angle (MFA) in their S2 sublayer, and this is to supply some lodging resistance [23][24] (Table 1). Fruit fibres like coir tend to protect seeds, so the germination could occur under optimal conditions. Their MFA is naturally designed to be between 30° and 50° to enhance toughness [24].

Table 1 Biochemical composition and microstructure of different plant fibres

Fibres	Cellulose [%]	Hemicelluloses [%]	Lignin [%]	Pectins [%]	MFA (°)	Ref.
Flax	64-85	11-17	2-3	1.8-2.0	10	[25][26]
Jute	61-75	13.6-20.4	12-13	0.6± 0.6	7-12	[27][28–30][26]
Kenaf	45-57	21.5	8-13	3-5	7-12	[27][29,32]
Coir	32-43	0.15-0.25	40-45	3-4	30-49	[27][33][26]

The biochemical composition of plant fibres also varies depending on their function and the environmental conditions during harvesting. Hemicellulose-rich (~15%) and pectin-rich (~2%) cell walls in flax are responsible for the major water sensitivity of those fibres, because of their amorphous structure and their large number of available hydroxyl groups [26]. More lignin-rich cell walls such as those present in jute (~13% [26]) and coir fibres (~45% [24]) provide resistance to diseases and to water [26][34][35].

The purpose of the present work is to establish a framework to design hygromorph actuators with improved performance and durability, and to discuss the potential application of these materials in simple smart assemblies. Here we present a plant fibre selection methodology based on their laminate hygroelastic properties and their theoretical curvature predicted by adapting a bimetallic theoretical model. The natural actuation ability of the fibres is discussed according to their microstructure and biochemical composition. The two best fibre candidates are then compared on the basis of their actuation performance. Mechanical and biochemistry tests are then used to investigate their durability in a severe environment. Finally, the potential of using Origami and Kirigami designs to develop hierarchical deployment systems based on HBCs is also discussed.

2 Materials and Methods

2.1 Materials selection

In this study flax, jute, kenaf and coir fibre composites have been selected as the actuating fibres, because these natural reinforcements exhibit quite a wide range of microstructural and biochemical properties. These fibres are also available as off-the-shelf industrial products in several countries, which makes feasible the concept of producing HBCs using local resources.

Flax fibres (*Linum usitatissimum*) were harvested in France and then dew-retted before being scotched and hackled. Unidirectional flax fibre tape (200 g/m² and 50 g/m²) was supplied by Lineo®. Jute fibres (*Corchorus capsularis* L) of the Tossa variety were supplied by Gold of Bengal. Kenaf fibres (*Hibiscus cannabinus L.)* were obtained from La Chanvrière de l'Aube, whereas Coconut or Coir fibres were provided by a car-seat padding manufacturer in Indonesia. The fibres were hand-hackled to form a unidirectional tape without any transverse.

Extruded and film-cast PP (PPC 3660 from Total Petrochemicals, 70g/m^2) and maleic anhydride (MA)-compatibilized polypropylene (MAPP) have been used.

2.2 Manufacturing of laminates and HBCs

Composite laminates with flax, jute, kenaf and coir fibres were then manufactured using a custom device that places fibre ribbons manually hackled and aligned before being hot pressed with MAPP films (20 bar, 190°C for 8 min). This approach reduces the numbers of defects and misalignments [36]. The fibre content within the HBC was set at 60% of volume [15]. The cooling rate was 15°C/min. The HBCs have been designed with a passive-to-active thickness ratio (n) of 0.2, which corresponds to the best curvature range previously observed for flax/MAPP HBCs.

Because the selected plant fibres exhibit anisotropic hygroelastic properties, their orientation within the HBC controls the global response. The orientation of flax fibres is 0° and 90° in the passive and active layers, respectively. This stacking sequence mimicks the topology present in the sclerenchyma fibres and and within the sclereids of a pine cone scale [37][38]. Five stripes with dimensions of 70 mm × 10 mm were then cut for the bending actuation experiments. By shaping the HBC with an elongated geometry (high length-to-width ratio) we were able to reduce the double (anticlastic) curvature [39]. In this way, we were also able to generate a cylinder as the actuated shape. The materials have then been stored under equilibrium conditions (T = 23°C and RH = 50%).

2.3 Swelling measurements

For each case, three square biocomposite samples of 50 mm X 50 mm have been cut. We have traced three lines longitudinally and transversally to the fibre orientation, to ensure that the swelling measurements were always performed at the same point. The results were then averaged arithmetically.

2.4 Water uptake

Bilayer samples have been immersed in deionized water until a constant weight was obtained (average time 24 hours). The samples have been periodically removed to be weighed and characterized. The percentage gain M_t at any time *t* has been calculated as:

$$M_t(\%) = \frac{W_t - W_0}{W_0} \times 100 \qquad \text{(Equation 1)}$$

Where W_t and W_0 are the weight of sample after water exposure and the weight of the dry material before immersion, respectively. The maximum moisture absorption M_∞ is calculated as the average value of five consecutive measurements. The desorption of the saturated samples was measured under laboratory conditions *(*RH = 50% and T = 23°C) by continuous recording the variations using a weighing device with 10^{-4} g accuracy.

2.5 Characterization of mechanical properties

The tensile properties of the wet biocomposites with their flax-fibre orientation set at 0° (E_L) and 90° (E_T) were measured separately on an MTS Synergie RT/1000 test machine at a controlled temperature (23°C) and at a crosshead speed of 1 mm/min (ISO 527-5). The mechanical tests have been performed only on samples that reached their saturation time. A 250-N force sensor was used to measure the load, and an axial extensometer with a nominal length of 25 mm (L_0) was used to measure the strain.

2.6 Analysis of the curvature

We estimated the bending curvature of the HBC during the immersion in deionized water by periodically taking photographs of one side of the clamped sample (HD Pro c920 Logitech®, 15 Megapixels). The samples have been fixed with a binder clip on a very small length of the sample to reduce the stress concentration over the bilayer. The image process analysis was performed using the ImageJ® software (National Institutes of Health, USA). Here, the deformed shape was assumed to be an arc of a circle and the curvature has been therefore measured by fitting the time history of the sample to a 'circle' function. The bending curvature (K) was calculated according to the radius of the fitted circle. The curvature was then normalized by the total thickness (t).

2.7 Leaching products: carbohydrate analysis

Three square samples (20 mm × 20 mm) have been cut from each biocomposite and immersed separately in 60 mL of water in an opaque container for 288 h. The samples have then been removed, and the solutions concentrated using a rotary evaporator. The obtained solutions have been deep-frozen for 12 h and freeze-dried for 24 h to recover the solid products. At the end of the process the obtained products have been weighed.

Neutral and uronic monosaccharides have been identified and quantified using HPAEC following a procedure described in [40], albeit with some slight modifications. The lyophilized extract fractions (approximately 5 mg) from flax or jute have been directly hydrolysed in 1.5 M H_2SO_4 for 2 h at 100°C. Contrary to previous protocols, the samples were not subjected to a pre-treatment in 12 M acid. The flax and jute samples have then been filtered, before being loaded onto an anion-exchange column. Detection was performed, and the samples were then eluted. The monosaccharide composition was analysed and quantified using 2-deoxy-D-ribose as the internal standard (100 µg/mL), as well as three concentrations of standard solutions (50, 200 and 500 µg/mL) of neutral (L-arabinose, D-glucose, D-xylose, D-galactose, and D-mannose) and uronic monosaccharides. The analyses were performed in triplicate from for every sample.

2.8 Scanning electron microscopy (SEM) observations

The samples have been sputter-coated with a thin layer of gold in an Edwards sputter coater and then inspected with a JEOL JSM 6460LV scanning electron microscope operated at an accelerating voltage of 20 kV.

3 Results and discussions

3.1 Selection of the actuating fibre

Figure 1a presents the evolution of the water uptake from different plant fibre laminates (flax, jute, kenaf and coir). Coir and kenaf fibres show a dramatic increase in water uptake compared to flax and jute. If we assume that the MAPP matrix is H_2O insensitive, the water could only enter through the cell wall, the fibre/matrix interface [20] and the interfibre areas [41], as well as through the fibre internal porous structure (lumen) [41]. As put in evidence by the SEM micrographs and by the image analysis, the internal porosity (i.e., free volume) of the kenaf (v_p = 13.8 ± 0.23%) and coir (v_p = 39.1 ± 0.7%) was very high compared to the one present in the flax (v_p = 0.1 ± 0.02%) and jute (v_p = 6.4 ± 0.17%) fibres. In addition, the kenaf and coir reinforcements exhibited a microstructure mainly composed by bundles of single fibres (Figure 1). These two features tend to promote large water transport characteristics

through the material, which may represent an advantage for the development of a moisture-induced actuator.

On the opposite, the water uptake for the flax and jute laminates is explained by their biochemical composition, with lower amounts of lignin (Table 1) and greater amounts of amorphous water-sensitive pectins and hemicelluloses.

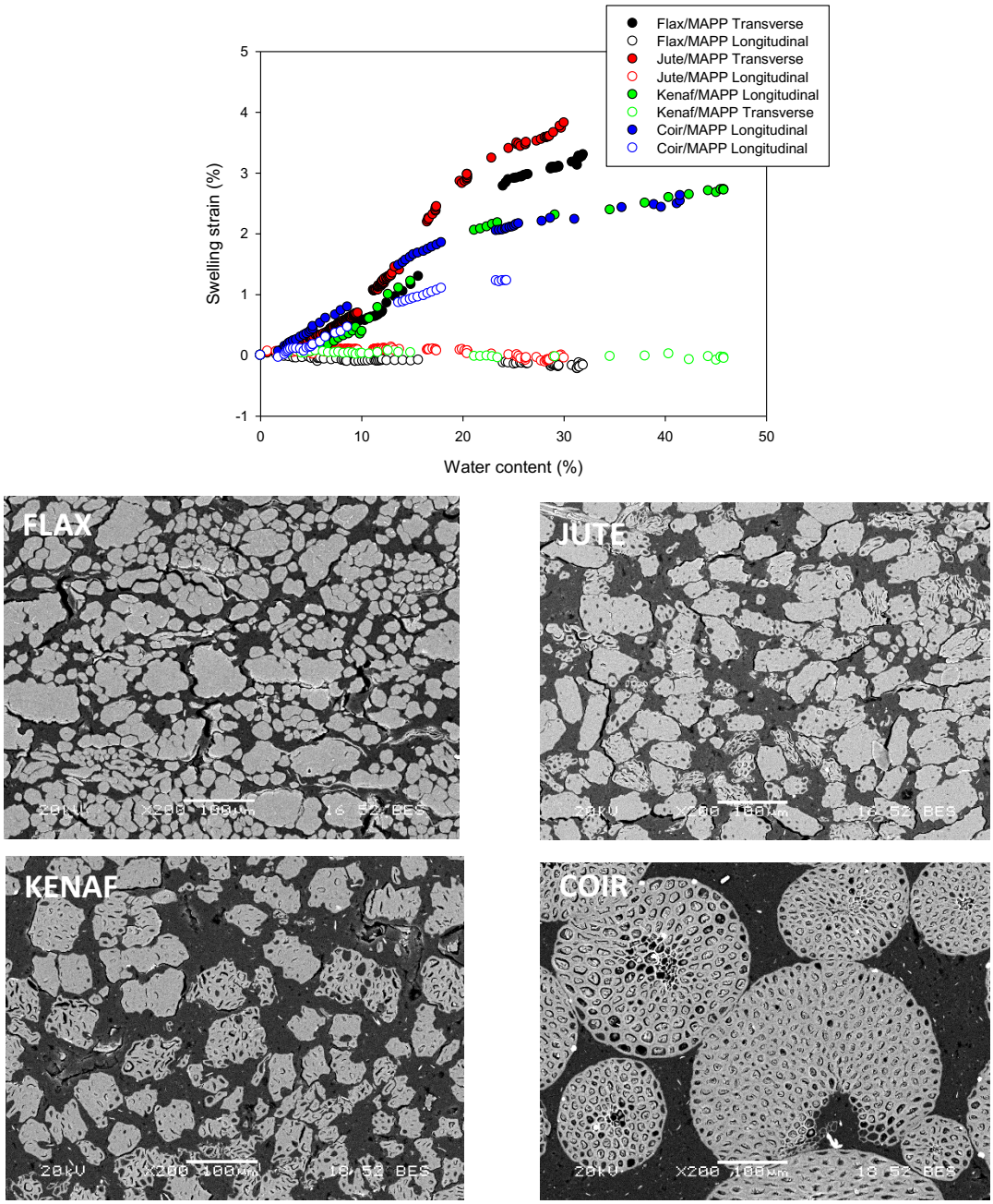

Figure 1 Evolution of the water uptake (a) and longitudinal and transverse swelling (b) as a function of the time and thickness for different plant fibre/MAPP biocomposites (Vf = 60%). (c) Influence of fibre topology on the laminate microstructure (c).

As a consequence of the water uptake, the plant fibre laminates tend to swell. The hygroscopic strains are in this case the drivers of the HBC actuation. For this reason it is important to carry out a careful examination on how the hygroelastic properties of the plant fibres affect the overall behaviour of the biocomposite actuators.

Flax, jute and kenaf laminates undergo a slightly negative or null longitudinal swelling deformation, whereas the coir laminates exhibit a higher deformation value, approximately equal to 1.5 ± 0.1%. The measurements of the Transverse strain swelling carried out during the stationary regime show that the flax and jute fibre composites feature the highest swelling ratios, with 3.3 ± 0.2% and 3.6 ± 0.6% for flax and jute respectively, followed by 2.7 ± 0.4% and 2.5 ± 0.4% for the kenaf and coir biocomposites. The differences in swelling between the laminates and their hygroscopic anisotropy are explained by the particular fibre microstructure at the cell-wall scale, i.e. the orientation of the microfibrils within the S2 cell-wall layer. The lower MFA in flax and jute leads to a higher radial swelling potential compared to the one present in coir laminates, which possess a higher MFA (Table 1). The biochemical composition also plays an important role in determining the swelling ability of fibres and, in determining therefore their actuation property. A high lignin content inhibits swelling, especially if a threshold of approximately 8% is reached [42]. Moreover, the fibre bundle division influences their swelling potential (Figure 1c). A higher fibre division promotes swelling [42], particularly in the case of flax. Thus, combination of microstructure, biochemical composition and fibre bundle division control the swelling ability of biocomposites.

A proper selection of plant fibres as actuators enables the development of a large anisotropic swelling strain required for the HBC design.

The transverse swelling kinetics highlights a clear peculiar behaviour in the flax fibre composites, which exhibit the fastest swelling amongst all the investigated composites. Fast rates of swelling are then featured by the kenaf, jute and coir composites (Figure 1a). A pectin-rich biochemical composition (table 1) and a lower free volume due to the low lumen size and consequently higher fibre cell-wall volume lead to faster swelling kinetics.

The plant fibre microstructural and biochemical composition, as well as the fibre bundle divisions, also tend to affect the mechanical properties of the laminates. Because of their high cellulose fraction and relatively low MFA, bast fibres (flax, jute and kenaf) show a greater longitudinal stiffness (or passive layer) than fruit fibres, i.e., coir laminates (Table 2).

Table 2 Mechanical properties of laminates in the dried state (RH = 50%) and wet state (after water immersion)

Materials	Dried state (RH = 50%)		Wetted state		Loss (%) E_{Lsec}/E_{Lsat}	Loss (%) E_{Tsec}/E_{Tsat}
	EL (MPa)	ET (MPa)	EL (MPa)	ET (MPa)		
Flax/MAPP	30,950 ± 2107	1791 ± 180	10,144 ± 1458	932 ± 146	67.2	48
Jute/MAPP	23,035 ± 2382	1786 ± 154	9304 ± 1006	936 ± 63	59.6	47.6
Kenaf/MAPP	11,477 ± 1434	2191 ± 129	4742 ± 504	922 ± 130	58.7	57.9
Coir/MAPP	3562 ± 514	1737 ± 63	1892 ± 299	907 ± 78	46.9	47.8

In the case of the flax laminates, the high fibre division and their filling ratios provide the highest tensile stiffness. The fibre effective properties were estimated by using a simple inverse rule of mixture; the results are similar to those reported in open literature [43][44].

The transverse properties of the laminates (or their active layer) are more sensitive to the matrix and fibre/matrix bond strength than to the topology of the fibre itself. Whatever their origin, these plant fibres tended to provide a similar range of transverse properties, despite their differences in fibre division and fibre surface chemistry.

The anisotropic ratio is known as the n-ratio (E_T/E_L or E_p/E_a) in Timoshenko equations [17], and it can be used to estimate how the actuator response evolves significantly among different classes of fibres. Flax exhibited the highest n-ratio (n_{flax} = 17.3) among the plant fibres considered in this work (n_{jute} = 12.9, n_{kenaf} = 5.2 and n_{coir} ≈ 2).

$$\Delta\kappa = \frac{\Delta\beta\Delta C\, f(m,n)}{h} \qquad \text{(Equation 2)}$$

$$f(m,n) = \frac{6(1+m)^2}{3(1+m)^2+(1+mn)\left(m^2+\frac{1}{mn}\right)} \qquad \text{(Equation 3)}$$

In (2) and (3), $m = \frac{t_p}{t_a}$, where t_p and t_a represent the passive layer and the active layer thicknesses, respectively. The parameter *n* is equal to $\frac{E_p}{E_a}$, where E_p and E_a represent the Young's modulus of the passive and active layers, respectively. The differential hygroscopic expansion between the active β_a and passive β_p layer is represented by $\Delta\beta$. The difference in water content between the immersion and drying steps is ΔC.

Other important parameters to design and produce reliable HBCs are the wetted mechanical properties, and the rate of loss between the dry and wet states. After water saturation the biocomposites exhibit a decrease of their longitudinal and transverse stiffness, mainly because of the plasticizing effect provided by the water on the fibres and the bond strength of the fibre/matrix interface [45]. Again, one needs to notice that MAPP is assumed here to be insensitive to water. Flax

fibre laminates appear to be the most sensitive, whereas their coir fibre counterparts exhibit a lower degradation of the longitudinal properties because of their high lignin content. Kenaf and jute laminates are here proposed as an intermediate solution, because the anisotropic ratios of the plant-fibre laminates only changes slightly from their initial configuration.

To develop a general framework to design an optimized HBC, we have used the Timoshenko bilayer theory because it provides a good approximation of the actuation curvature for the assumed strip geometry [13][14][15]. The theoretical curvature was estimated from the hygroelastic properties measured through the mechanical characterization, whereas the parameter β was expressed as the swelling coefficient (ε/Δm) or swelling deformation (%) (Table 3).

Table 3 input parameters and theoretical actuation (curvature) of HBC with different fibre species

Materials	Δβ = βa - βp (ε/Δm)	ε_{hygro}= $\varepsilon_{hygro\ (a)}$ - $\varepsilon_{hygro\ (p)}$ (%)	n = Ep/Ea (wet state)	K (mm^{-1})	K.thickness
Flax/MAPP	0.107	3.55	10.9	0.095	0.044
Jute/MAPP	0.11	3.70	9.95	0.094	0.043
Kenaf/MAPP	0.07	2.80	9.1	0.088	0.040
Coir/MAPP	0.03	1.10	2.1	0.027	0.013

Compared to synthetic actuators, these biocomposites produce a specific actuation strain and stress comparable to the one of SMAs, hydraulic and piezoelectric polymers, but lower than that of SMPs and other pneumatic counterparts.

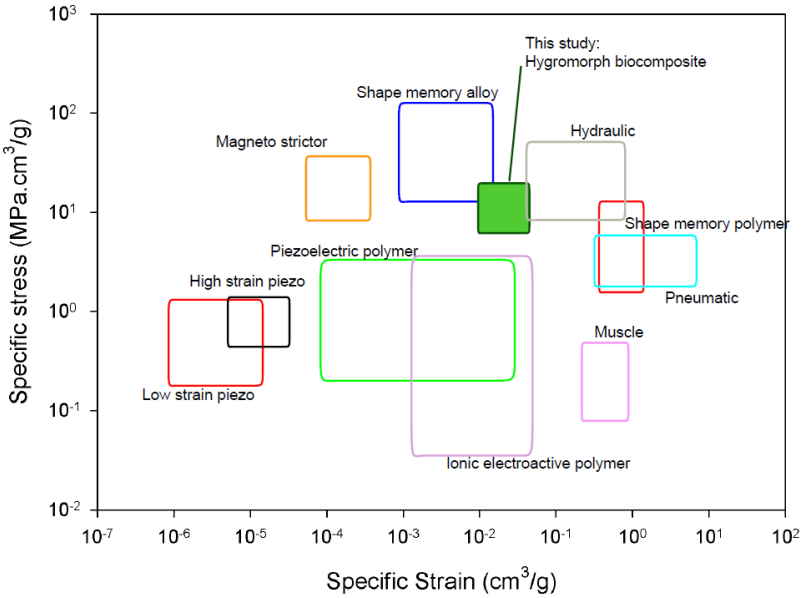

Figure 2 Active materials specific performance based on ref [3][46][47][48], and this work.

On the basis of the aforementioned results, the plant fibres exhibit strong potential for their use as HBCs in shape morphing, and also to provide some blocking force as evidenced elsewhere [11]. Amongst the investigated fibres, flax and jute are the best actuating reinforcements in high-performing HBCs with the highest curvature. The kenaf and coir/MAPP are clearly less promising, and have not been further studied in this work. A following systematic actuation analysis (including the first sorption/desorption cycle) and hygromechanical fatigue have been only carried out on the flax and jute HBCs.

3.2 Actuation performance of the flax and jute HBCs

3.2.1 Analysis of actuation behaviour at the first sorption/desorption cycle

Before testing the initial water content of the HBCs was determined because a variation in the water fraction triggers actuation. We also performed gravimetric analyses before and after the thermocompression, and after storage at 50% RH. Because the MAPP is insensitive to water the initial moisture content in the flax and jute fibres was relatively high (10.3 ± 0.5% and 8.4 ± 1.8%, respectively). During the process the water content was greatly reduced because of vaporisation (5.3 ± 0.4% for the flax laminate and 1.7 ± 0.1% for the jute laminate). The moisture content at which the bilayers are assembled influences the range of the actuation curvatures [49]; in the present case it might be difficult to produce an increase of the amount of water within the fibres, as Hosltov *et al.* [49] did by assembling moisturized wood layers. Nevertheless, in future works one may consider the use of a mould to set the initial shape and widen the deformation capability of these HBCs. The storage at RH = 50% and 23°C until a constant weight was reached did not allow the recovery of the initial moisture content in the single fibres (the water % in flax was 8.7 ± 0.3 and in kenaf equal to 5.4 ± 0.25). The lack of recovery of the initial moisture content is due to the potential biochemical modification of the fibres, and the stress state inside the laminate.

After immersion in the deionized water, the flax and jute MAPP biocomposite actuators absorbed some substantial and similar amounts of water, and all exhibited similar kinetics. The water amount at saturation in the actuators and the unidirectional laminates differs, because of the hygroscopic stresses developed in the [0, 90] asymmetric laminates. This difference could reduce the free volume available (Figure 1a). Both the flax and the jute MAPP actuators exhibited a hysteretic behaviour between sorption and desorption, with faster desorption. A major difference between the flax and jute fibres appears at the end of the desorption. The jute/MAPP actuator maintained a water content of approximately 2%, whereas the flax/MAPP exhibited a weight loss with a negative weight variation (Figure 3a).

The actuation modes of the two actuators were quite similar during the sorption step (Figure 3b). In this case we can observe two distinct phases: an initial quick response, followed by a stabilisation after 60 mins of immersion. The flax and jute fibres had similar maximal actuations (ΔK.thickness = 0.034 ± 0.001 for jute/MAPP and 0.037 ± 0.006 for flax/MAPP) in a similar time step of 60 minutes. Although the curvature range was rather well predicted, the theoretical predictions slightly overestimated the range by 10%-15%.

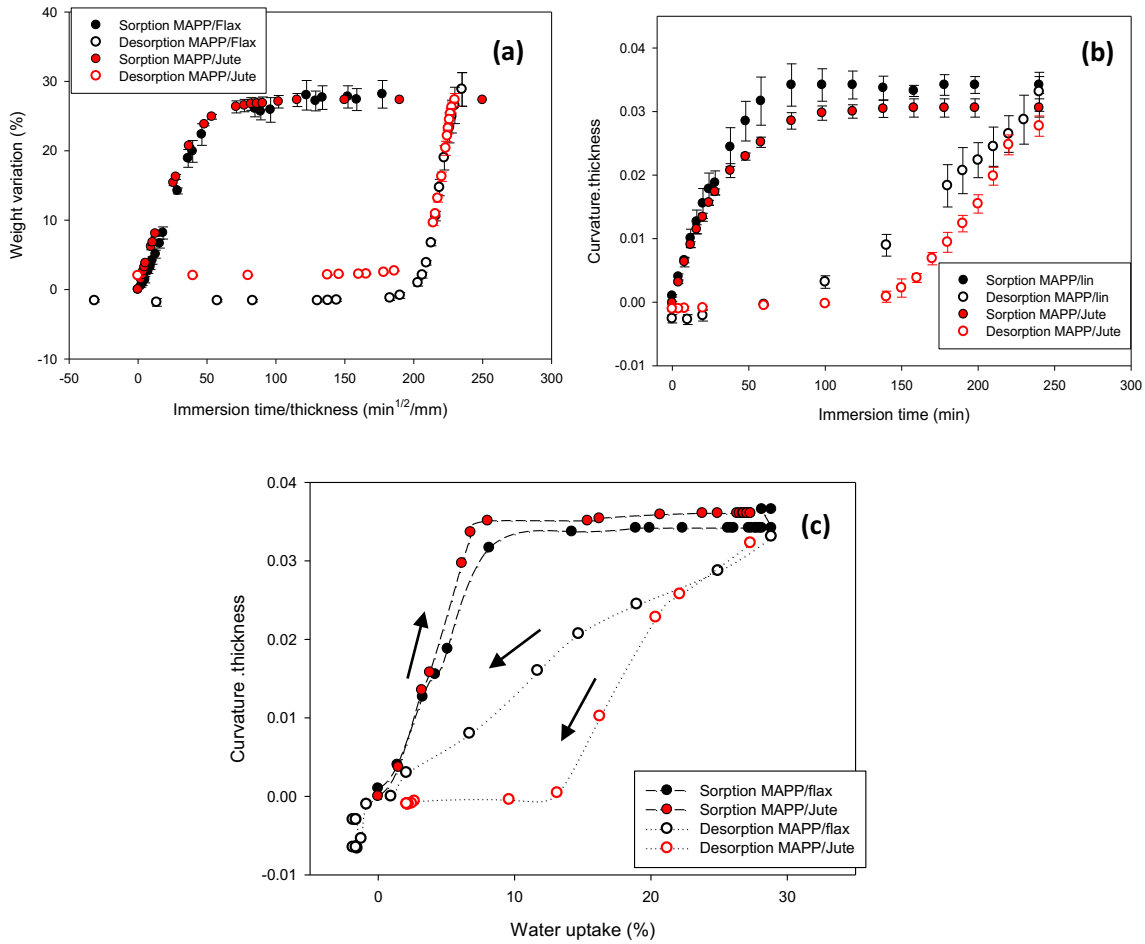

Figure 3 Evolution of the weight variation during sorption/desorption of the flax and jute HBCs (a); evolution of the curvature and reversibility (b); and actuation behaviour as a function of the weight variation (water content) (c).

This overestimation of the curvature can be attributed to: (i) the boundary conditions, (ii) the presence of a hygroscopic stress state, (iii) the accuracy of the measured β value and (iv) the layer thickness, and (v) an incomplete description of the mechanical behaviour (i.e., the Poisson's ratio and anisotropic properties of the plies, which were not taken into account in the model).

The actuation speeds were of the flax and jute HBCs were similar, and varied from 5×10^{-4} to 8×10^{-4} min^{-1}. Compared with other materials such as SMAs, the HBCs exhibit a slower morphing speed

because of the water transport process; therefore, further improvement strategies such as enhancing the mechanical instability [50][51][52][53][54] or identifying proper applications should be pursued.
During the desorption the flax and jute actuators showed both a hysteretic behaviour and a slower straightening compared to the moisture-absorption-induced curvature case. This behaviour was especially evident in the flax systems (Figure 3b). The jute/MAPP will therefore result in faster actuators than the flax/MAPP. Both systems however reverted to their initial position within a similar time scale, which is an important point for the design of an actuator. The reversibility remains indeed a topic of considerable interest for the development of these actuators, and it is a potential drawback for plant-fibre-based systems [14][15]. Our HBC actuators were actually more than reversible. A slight negative curvature was observed for the jute/MAPP and the flax/MAPP, with 3.1 ± 1.1% and 8.1 ± 1.8% of the maximal curvature, respectively. A more substantial version (~50%) of this phenomenon has been however observed in wood/glass fibre composites with thin active layers assembled under room temperature and RH conditions [49]. The lower negative curvature values for the flax and jute could be due to the low initial water content inside the plant fibres during the assembly of the HBC, because of the melting of the polymer. Holstov *et al.* [49] have also reported that the active layer could shrink to dimensions smaller than its initial ones after one wetting/drying cycle. This point must be further investigated for the an improved and practical use of HBCs.
Apart from the immersion time, the moisture is another major driver for the actuation of HBCs, and it depends on the water content (Figure 3c). The fibre morphology plays therefore an important role in the HBCs response (Figure 1b), along with the lumen size and its biochemical composition (Table 1). The jute and flax systems again exhibited similar responses as a function of the water content during sorption, but a significant hysteresis loop was observed during desorption. This type of hysteresis may be due to the lignin content [55] and the damage mechanism that modifies the water transport. This point will be further discussed in the following section.

The diversity of the plant fibres with respect to the biochemical composition and the microstructure enables to design HBCs by using local feedstocks (European or Asiatic, for instance). A proper selection of fibres like jute and flax could supply an actuator with improved response and reversibility. In addition, unlike coir and kenaf fibres, flax and jute are currently available in composite fabrics; this would enable the efficient design of the HBCs by using more mechanically stable and technologically refined natural reinforcements.

3.2.2 Effect on hygromechanical fatigue

In a real environment HBCs could be subjected to cyclic variations of their moisture content. To this end, we have performed cycles of immersion/desorption at RH = 50% in order to assess the particular

behaviour of the hygromorph composites. The flax/MAPP exhibited a loss of curvature return (–20%) after 40 cycles (Figure 4a).

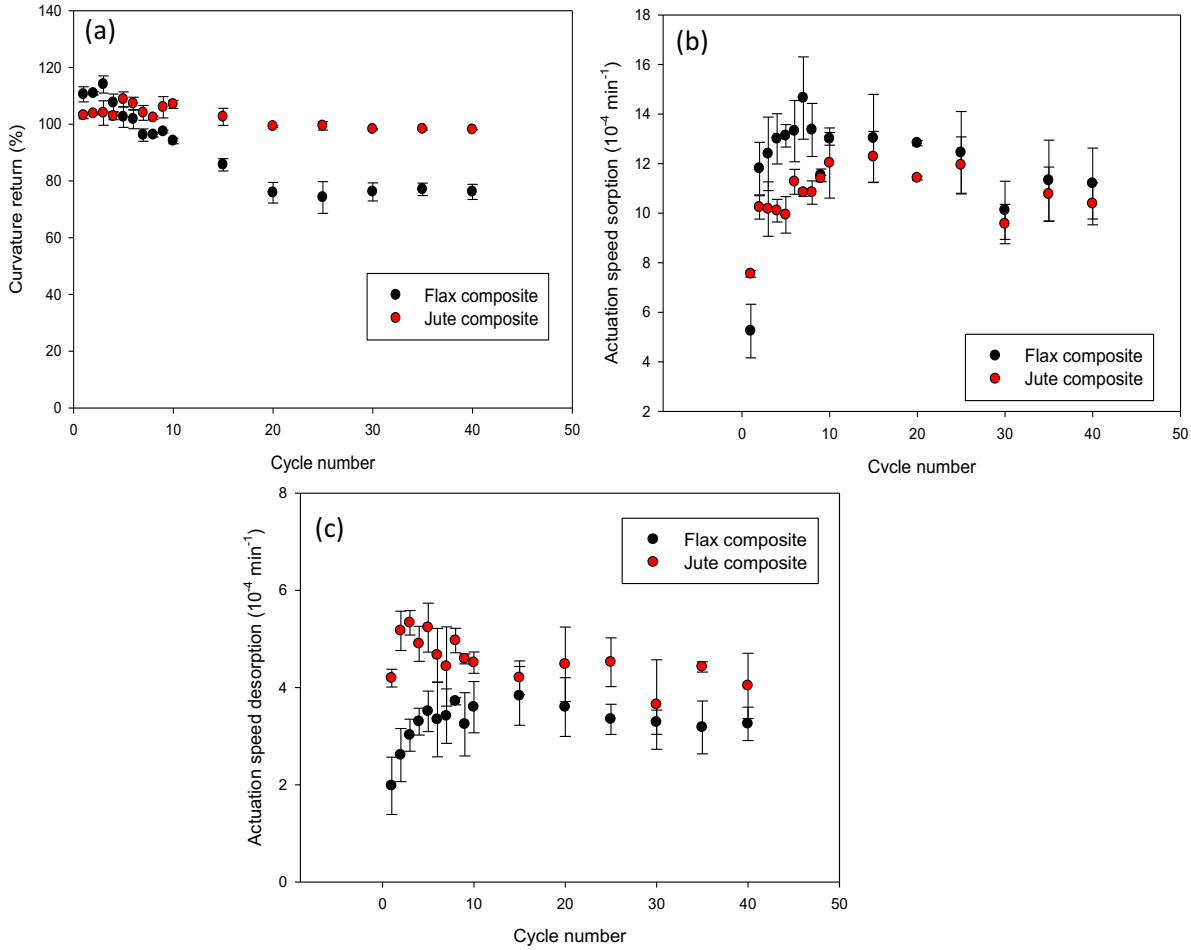

Figure 4 Influence of the fibre nature on the curvature return (a) and on the actuation speed at sorption (b) and desorption (c) as a function of sorption/desorption cycles.

Some previous work has however highlighted a more dramatic degradation of the actuation [15] (-40% over 10 cycles) because of the boundary conditions. The clamping length in the present series of tests was actually between 2 mm and 3 mm, and not the 10 mm used in previous works. This shorter clamping length leads to stress concentration and overall loss of durability. This information might be important to design future HBC assemblies. Unlike the flax/MAPP ones, the jute actuators however exhibited some interesting durable performance in severe environments, by providing an almost constant response during cycling (Figure 4a). The change in actuation speed was also influenced by the type of plant fibre. The jute/MAPP systems exhibited a weaker increase in actuation speed by a factor of 1.5, against the more remarkable factor of 5 observed in the flax/MAPP HBCs (Figure 4b). For the two types of actuators, it is possible to observe that the initial speed increase is followed by a stabilization at higher cycle numbers. This phenomenon can be attributed to the interfacial porosity

that arises from the fibre swelling/shrinking cycles. The porosity will subsequently reduce the permeability and will allow a faster water transport inside the laminate [56]. This behaviour has also been observed in paper architectures for 4D deployment [57] and plant fibre composite laminates [56]. During the desorption the type of fibre selected strongly affects the behaviour of the actuator, and the jute-based ones consistently exhibit a faster straightening actuation with a constant response.

The aforementioned results demonstrate a general weak dependency of the actuation speed for the jute actuators. Contrary to what established previously, the formation of the porosity is not the major degradation mechanism of the HBCs, as indicated by the jute/MAPP exhibiting a constant curvature amplitude.

The analysis of the released matter—more specifically, sugar—highlights that the leachate amounts differ for the flax and jute actuators (-3.6% for flax and -0.6 for jute/MAPP), and this is consistent with data published elsewhere [24]. The jute fibre has higher lignin content than flax, and the lignin is well known to be water resistant. The major difference between flax and jute released products is the monosaccharide rhamnose content from rhamnogalacturonans (RGI and II). These components belong to the pectin family and explain the variation in intensity of the leaching process. In the case of flax, these polysaccharides can be localized into the middle lamellae, the cellular junctions and the primary cell walls. These parts correspond to the fibre/matrix and fibre/fibre interfacial regions (internal to the bundles). This localization implies the creation of an interfacial porosity and split of the bundles of fibres, which result in a reduced hygroscopic loading transfer [20]. In addition, rhamnogalacturonans can also be localized in secondary cell walls and their leaching induces a loss of the cell-wall stiffness [19]. Polysaccharide leaching is thus the first step of degradation, which explains the hygromechanical fatigue behaviour of the flax/MAPP. In the case of the jute actuators, the concentrations of the leaching products were very low, but their origin within the cell wall was far from straightforward to identify. To the best of our knowledge, in open literature there is an evident lack of comprehensive understanding about the precise microstructural and biochemical description of the jute fibres. An appropriate knowledge of both the microstructure and the biochemical composition of these fibres is important to enable their selection as a swelling agent for the design of HBCs. Plant fibres with a high anisotropic ratio (E_L/E_T) and rich lignin composition must be selected to properly design HBCs capable of being immersed in a severe environment.

3.3 How to use HBCs as building blocks for deploying structures

Planar HBCs are essentially produced by thermocompression. The question arises as to how to use and develop HBC structures capable of complex deployment.

Origamis (*oru*, ' fold', and *kami*, 'paper') are widely employed to develop autonomous self-folding systems [7]. If used within Engineering Origami, HBCs may be capable of massive folding, i.e., bending [7]. A crease pattern would influence the complex deployment of the HBC sheet. HBCs with a 60% flax or jute fibre/MAPP matrix have a maximal curvature that allows a minimal curvature radius of approximately 12 mm. At curvatures beyond this radius, the crease represents a permanent deformation that exceeds the elastic limit of the material, which corresponds to the onset of damage for a laminate. In addition, HBCs have low strain at rupture ($\varepsilon r_{flax/MAPP}$ = 1.00 ± 0.22% and $\varepsilon r_{jute/MAPP}$ = 0.74 ± 0.14%), which reduces their magnitude of folding without damage and precludes their use in such origami design processes. Another type of Origami engineering is the hinge-type one. In this case, a hygroscopically active biocomposite can play the role of an active hinge that connects facets of passive materials. Figure 5a presents the evolution of a hinge-type Origami prototype in which an HBC is used as active hinges and PLA polymer is used as passive facets before and after water immersion. Hinge-less square sheets with a curved crease pattern could yield a specific folding and create a 3D shape [58].

a)

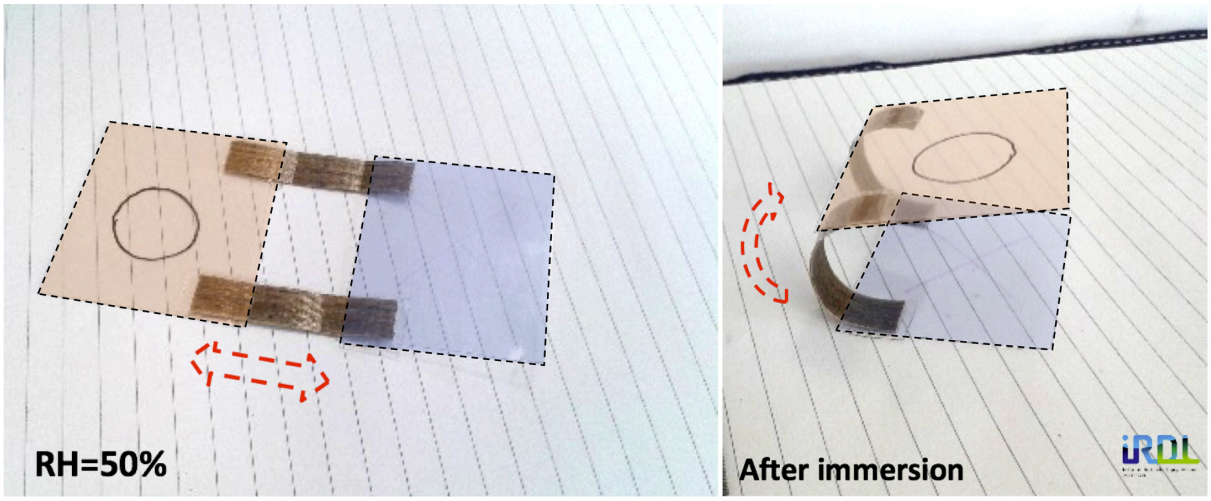

(b)

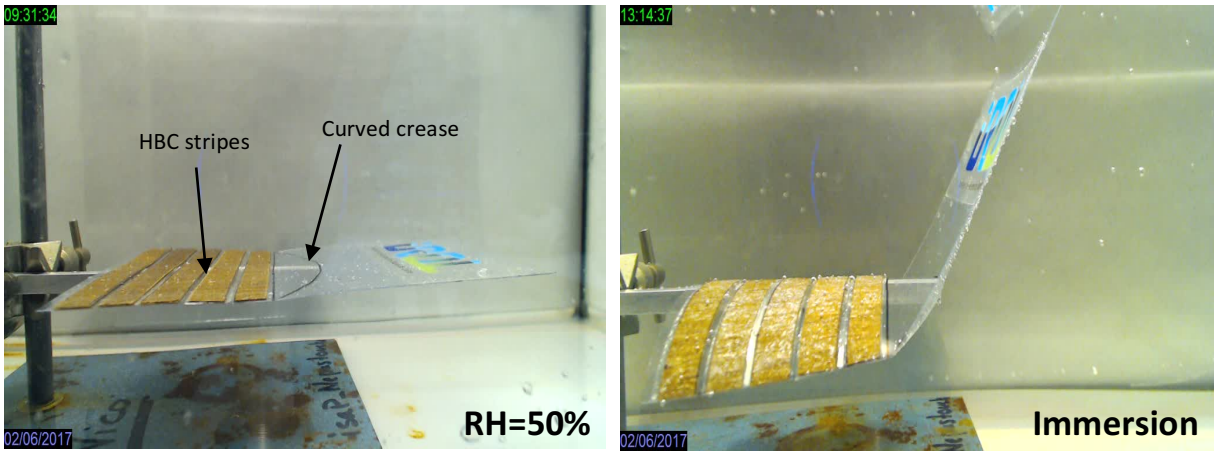

Figure 5 Example of Hygromorph biocomposites used as : Hinge type origami (a) and a simple deployable structure based on curved line folding (b)

Both elements of the sheets are constrained by each other because of the curved line. Thus, a small uniaxial bending will force the thin shell element to bend with a reverse curvature. The exploitation of the anisotropic behaviour of the HBCs and their placement on the backbone element during the planar state the generation of a continuous bending of this element during sorption (Figure 5b, RH = 50%). The forces and the moment are therefore transmitted through the crease to the adjacent face and trigger autonomous self-snapping.

During actuation the HBC did not reach however a curvature comparable to the one present in stripes systems previously tested (Figure 5b), because of the mechanical constraint induced by the crease pattern. The viscoelastic behaviour of the PP matrix may have additionally promoted creep. The blocking force and the bending moment of the HBCs must be therefore systematically characterized so that the formulation and m-ratio ($t_{active}/t_{passive}$) can be optimized. To this purpose, sets of useful data can be found elsewhere [11].

Another geometrical effect is currently used to enhance the deployability of structures. The Kirigami concept (*kiri* – 'to cut' and *gami* – 'paper'), which involves a dedicated cutting pattern, enables the out-of-plane deformation of 2D sheets so that 3D deployment is possible through a 'Kirimimetic' approach (Figure 6) [6].

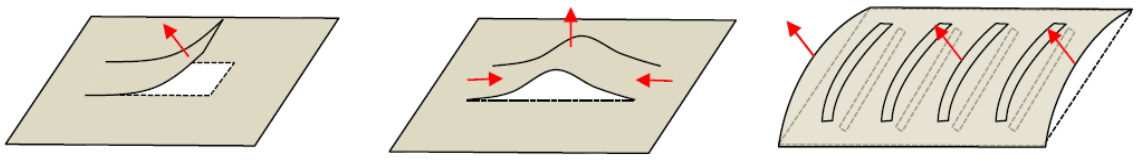

(a) (b) (c)

Figure 6 Fundamental Kirigami out-of-plane deformations: bending into the 3rd dimension (a), bucking out of plane (b), and whole-sheet bending by selective sectioning (c).[6]

Kirigami is often applied to passive materials; however smart materials (electro-active, SMA, SMP) have been also recently used to develop self-deploying structures [1][6][59]. In a similar way, we have generated laser-cut HBCs with different simple cutting patterns that exhibit bending and twisting responses from a planar biocomposite sheet (Figure 7a and b). The laser cutting also enables the creation of patterns with tiny cuts (2 mm in width), so that moisture-actuated membranes can be manufactured (Figure 7c).

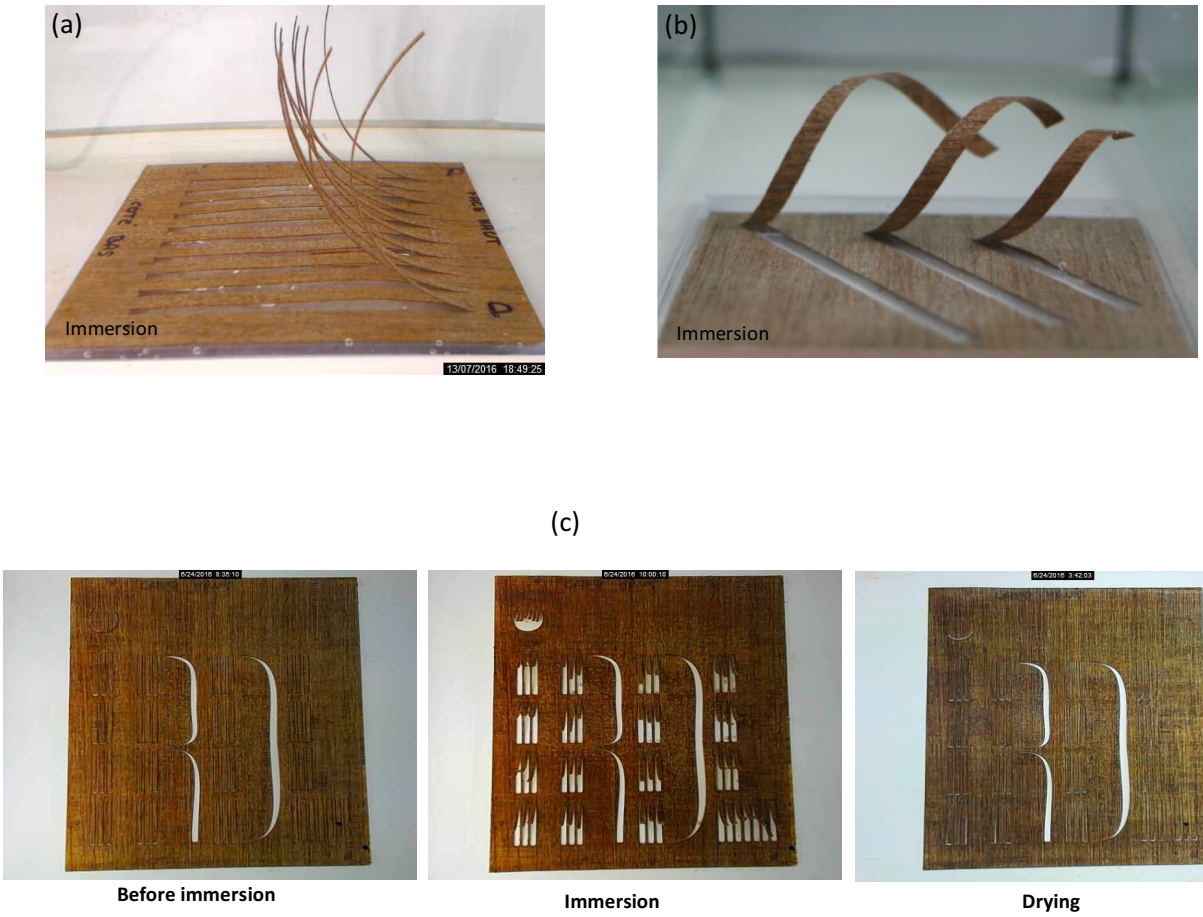

Figure 7 Kirigami design for HBCs: simple longitudinal cut patterns (a), diagonal (b) and IRDL'laboratory logos (c). [2]

4 Conclusions

In the present article we have developed guidelines for the design of HBC actuators with improved performance and durability in severe environments under cyclic loading and stimulus. Plant fibres serve as naturally actuating fibres because of their moisture sensitivity. We have also proposed a plant fibre selection methodology based on the Timoshenko bimetallic equations to evaluate the theoretical actuating response (curvature) and characterized the hygroelastic properties of plant fibres (flax, jute, kenaf, and coir)/MAPP laminates. Their actuation potential appears to be directly controlled by their fibre microstructure (cellulose MFA and lumen size) and biochemical composition (pectins, hemicelluloses and lignin). Plant fibres have been therefore used as natural actuating fibres, and their selection will lead to a wide range of potential HBCs with low environmental footprints. Jute and flax fibres appear to be the best candidates for the design and manufacturing of HBCs. Flax/MAPP and jute/MAPP were tested in water immersion/drying cycles (RH = 50%) for over 40 cycles. The actuating behaviours of the HBCs were similar during the sorption step (amplitude and speed), however differed during desorption because of the combined effect of the lumen size, fibre division and biochemical composition on the desorption mechanism. During the hygromechanical fatigue tests the jute/MAPP HBC clearly showed an improvement in durability compared to flax HBCs, with a constant actuation performance over the complete cycles. The higher lignin content of the jute reduces the amount of sugar released and thus reduces the degradation kinetics.

Beyond stripe samples, HBCs were used to trigger the deployment of adaptive structures. Origami and Kirigami techniques currently used to develop smart material systems were applied to design HBCs, and confirmed their potential applications in moisture-induced self-shaping systems. Although essentially triggered by a moisture variation, the HBCs and their actuating plant fibres are also sensitive to temperature. Combining these HBCs with SMPs could therefore enlarge their response spectrum and design envelope.

5 References

[1] Neville. RM, Chen. J, Guo. X, Zhang. F, Wang. W, Dobah.Y, Scarpa.F, Leng. J and PH. A kirigami shape memory polymer honeycomb concept for deployment. Smart Mater Struct 2017;5:05LT03.

[2] Rossiter. J, K. Takashima, F Scarpa PW. Shape memory polymer hexachiral auxetic structures with tunable stiffness. Smart Mater Struct 2014;23:045007.

[3] Peraza-Hernandez EA, D. J Hartl, R. J Malak Jr and DCL. Origami-Inspired Active Structures: A Synthesis and Review. Smart Mater Struct 2014;23:094001.

[4] Tachi T. Simulation of Rigid Origami. Origami 2009;4:175–87.

[5] Nojima T and Saito K. Development of newly designed ultra-light core structures.

JSME Int J Ser A 2006;49:38–42.

[6] Rossiter. J SS. Kirigami design and fabrication for biomimetic robotics. Bioinspiration, Biomimetics, Bioreplication, Proc SPIE 2014;9055.

[7] Peraza-Hernandez. EA, DJ Hartl, RJ Malak Jr and DL. Origami-Inspired Active Structures: A Synthesis and Review. Smart Mater Struct 2014;23:094001.

[8] Ionov L. Hydrogel-based actuators: possibilities and limitations. Mater Today 2014;17:494–503.

[9] Hamedi . MM, VE. Campbell , P Rothemund FG, DC. Christodouleas , JF Bloch and GW. Electrically Activated Paper Actuators. Adv Funct Mater 2016;26.

[10] Gîder. F, A. Ainla, J. Redston, B. Mosadegh, A. Glavan, TJ. Martin AGW. Paper-Based Electrical Respiration Sensor. Angew Chemie 2016;55:5727–32.

[11] Le Duigou A, Castro M. Evaluation of force generation mechanisms in natural, passive hydraulic actuators. Sci Rep 2016;18105.

[12] Reyssat E, Mahadevan L. Hygromorph: from pine cone to biomimetic bilayers. J R Soc 2009;6:951–7.

[13] Le Duigou A, Castro M, Bevan R, Martin N. 3D printing of wood fibre biocomposites: From mechanical to actuation functionality. Mater Des 2016;96:106–14. doi:10.1016/j.matdes.2016.02.018.

[14] Le Duigou A, Castro M. Moisture-induced self-shaping flax-reinforced polypropylene biocomposite actuator. Ind Crops Prod 2015;71:1–6. doi:10.1016/j.indcrop.2015.03.077.

[15] Le Duigou, A., Castro M. Hygromorph BioComposites : Effect of fibre content and interfacial strength on the actuation performances. Ind Crop Prod 2017;99:142–9.

[16] Azwa ZN, Yousif BF, Manalo AC, Karunasena W. A review on the degradability of polymeric composites based on natural fibres. Mater Des 2013;47:424–42. doi:http://dx.doi.org/10.1016/j.matdes.2012.11.025.

[17] Timoshenko S. Analysis of bi-metal thermostats. J Opt Soc Am 1925;11:233–55.

[18] Reyssat E, Mahadevan L. Hygromorphs: from pine cones to biomimetic bilayers. J R Soc Interface 2009;6:951–7. doi:10.1098/rsif.2009.0184.

[19] Le Duigou A, Bourmaud A, Baley C. In-situ evaluation of flax fibre degradation during water ageing. Ind Crops Prod 2015;70:204–10. doi:10.1016/j.indcrop.2015.03.049.

[20] Le Duigou A, Davies P, Baley C. Exploring durability of interfaces in flax fibre/epoxy micro-composites. Compos Part A Appl Sci Manuf 2013;48:121–8. doi:10.1016/j.compositesa.2013.01.010.

[21] Bag, R. Beaugrand, J., Dole, P., Kurek B. Treatment of chenevotte, a co-product of industrial hemp fiber, by water or hydrochloric acid: impact on polymer mobility in

the lignified cell walls. J Wood Sci 2012;58:493–504.

[22] Le Duigou A, Davies P, Baley C. Environmental impact analysis of the production of flax fibres to be used as composite material reinforcement. J Biobased Mater Bioenergy 2011;5. doi:10.1166/jbmb.2011.1116.

[23] Hearle J. The fine structure of fibers and crystalline polymers III. J Appl Polym Sci 1963;7:1207–23.

[24] Mussig J. Testing methods for measuring physical and mechanical fibre properties (plant and animal fibres). In: John Wileys & Sons, editor. Ind. Appl. Nat. fibres Struct. Prop. Tech. Appl., 2010, p. 269–309.

[25] Lefeuvre A, Duigou A Le, Bourmaud A, Kervoelen A, Morvan C, Baley C. Analysis of the role of the main constitutive polysaccharides in the flax fibre mechanical behaviour. Ind Crops Prod 2015;76:1039–48. doi:10.1016/j.indcrop.2015.07.062.

[26] Hill CAS, Norton A, Newman G. The water vapor sorption behavior of natural fibers. J Appl Polym Sci 2009;112:1524–37. doi:10.1002/app.29725.

[27] Bismarck A, Mishra S, Lampke T. Mohanty AK, Mishra M DL. Plant fibers as reinforcement for green composites. Nat Fibers, Biopolym Biocomposites Boca Rat CRC Press 2005.

[28] Pickering K. Properties and Performance of Natural-Fibre Composites. Elsevier; 2008.

[29] Monti A, Alexopoulou E, editors. Kenaf: A Multi-Purpose Crop for Several Industrial Applications. London: Springer London; 2013.

[30] Bledzki AK, Gassan J. Composites Reinforced with Cellulose Based Fibres. Prog Polym Sci 1999;24:221–74.

[31] “Effective Properties of Randomly Oriented Kenaf Short Fiber Reinforced” by Dayakar Naik L. n.d.

[32] Akil HM, Omar MF, Mazuki AAM, Safiee S, Ishak ZAM, Abu Bakar A. Kenaf fiber reinforced composites: A review. Mater Des 2011;32:4107–21. doi:10.1016/j.matdes.2011.04.008.

[33] Faruk O, Bledzki AK, Fink H-P, Sain M. Biocomposites reinforced with natural fibers: 2000–2010. Prog Polym Sci 2012;37:1552–96. doi:10.1016/j.progpolymsci.2012.04.003.

[34] Vance C, Kirk T, Sherwood R. Lignification as a mechanism of diease resistance. Ann Rev Phytopathol 1980;18:259–88.

[35] Muraille L, Pernes M, Habrant A, Serimaa R, Molinari M, Aguié-Béghin V, et al. Impact of lignin on water sorption properties of bioinspired self-assemblies of lignocellulosic polymers. Eur Polym J 2015;64:21–35. doi:10.1016/j.eurpolymj.2014.11.040.

[36] Coroller G, Lefeuvre A, Le Duigou A, Bourmaud A, Ausias G, Gaudry T, et al. Effect of flax fibres individualisation on tensile failure of flax/epoxy unidirectional composite.

Compos Part A Appl Sci Manuf 2013;51. doi:10.1016/j.compositesa.2013.03.018.

[37] Harlow W, Coté W, Day A. The opening mechanism of pine cone scales. J For 1964:538–40.

[38] Dawson C, Vincent J, Rocca A. How pine cone open. Nature 1997;390:668.

[39] Alben S, Balakrisnan B, Smela E. Edge Effects Determine the Direction of Bilayer Bending. Nanoletter 2011;dx.doi.org.

[40] Beaugrand. J, M. Nottez JK and AB. Multi-scale analysis of the structure and mechanical performance of woody hemp core and the dependence on the sampling location. Ind Crops Prod 2014;60:193–204.

[41] Stuart T, McCall RD, Sharma HSS, Lyons G. Modelling of wicking and moisture interactions of flax and viscose fibres. Carbohydr Polym 2015;123:359–68. doi:10.1016/j.carbpol.2015.01.053.

[42] Roy M, Sen M. The swelling of jute fiber in water (transverse swelling). J Text Inst Trans 1952;43:396–401.

[43] Yusoff RB, Takagi H, Nakagaito AN. Tensile and flexural properties of polylactic acid-based hybrid green composites reinforced by kenaf, bamboo and coir fibers. Ind Crops Prod 2016;94:562–73. doi:10.1016/j.indcrop.2016.09.017.

[44] Le Duigou A, Bourmaud A, Gourier C, Baley C. Multi-scale shear properties of flax fibre reinforced polyamide 11 biocomposites. Compos Part A Appl Sci Manuf 2016;85:123–9. doi:10.1016/j.compositesa.2016.03.014.

[45] Le Duigou A, Bourmaud A, Davies P, Baley C. Long term immersion in natural seawater of Flax/PLA biocomposite. Ocean Eng 2014;90:140–8. doi:10.1016/j.oceaneng.2014.07.021.

[46] Kumar. PK DL. Introduction to Shape Memory Alloys. Shape Mem Alloy 2008;DOI: 10.10.

[47] Huber. JE FN and MA. The selection of mechanical actuators based on performance indices. Proc R Soc L A 1997;453:2185–205.

[48] Leng. S, X Lan, Y Liu SD. Shape-memory polymers and their composites: Stimulus methods and applications. Prog Mater Sci 2011;56:1077–135.

[49] Holstov A, Bridgens B, Farmer G. Hygromorphic materials for sustainable responsive architecture. Constr Build Mater 2015;98:570–82. doi:10.1016/j.conbuildmat.2015.08.136.

[50] Hu. N and R. Burgueno. Buckling-induced smart applications: Recent advances and trends. Smart Mater Struct 2015;24:063001.

[51] Coulais C, Overvelde JTB, Lubbers LA, Bertoldi K van HM. Discontinuous Buckling of Wide Beams and Metabeams. Phys Rev Lett 2015;115.

[52] Kang SH, Raney J, Wang P, Fang L, Candido F, Lewis J BK. Multistable Architected Materials for Trapping Elastic Strain Energy. Adv Mater 2015;27:4296.

[53] Mosadegh. B, P. Polygerinos, C. Keplinger, S. Wennstedt, RF. Sheperd, U. Giupta, J. Shim, K. Bertholdi CW and GW. Pneumatic networks for soft robotics that actuate rapidly. Adv Funct Mater 2014;24:2163–70.

[54] Chen, Z., Guo, Q., Majidi, C., Chen, W., Srolovitz, D. J., & Haataja MP. Nonlinear geometric effects in mechanical bistable morphing structures. Phys Rev Lett 2012;109:114302.

[55] Xie. Y, CAS. Hill, Z. Jalaludin, SF. Curling RDA, AJ. Norton GN. The dynamic water vapour sorption behaviour of natural fibres and kinetic analysis using the parallel exponential kinetics model. J Mater Sci 2011;46:479–89.

[56] Newman RH. Auto-accelerative water damage in an epoxy composite reinforced with plain-weave flax fabric. Compos Part A Appl Sci Manuf 2009;40:1615–20. doi:10.1016/j.compositesa.2009.07.010.

[57] Mulakkal, M. C., Seddon, A. M., Whittell, G., Manners, I. and Trask RS. 4D fibrous materials:characterising the deployment of paper architectures. Smart Mater Struct 2016;25:095052.

[58] Demaine. ED, ML. Demaine, D Koschitz TT. Curved Crease Folding a Review on Art, Design and Mathematics. Proc IABSE-IASS Symp 2011.

[59] Sareh. S and J Rossiter. Kirigami artificial muscles with complex biologically inspired morphologies. Smart Mater Struct 2013;22:014004.